IMPURITY DYNAMICS IN TOKAMAK LIKE MAGNETIC CONFIGURATION WITH X-POINT

A.O. Moskvitin[1], A.A. Shishkin[2,1]
[1]Department of Physics and Technology,
Kharkiv "V.N.Karazin" National University, Kharkiv, Ukraine;
[2]National Science Center "Kharkov Institute of Physics and Technology", Kharkiv, Ukraine
E-mail: Anton.Moskvitin@gmail.com

Expressions for plasma flow velocities are obtained in invariant form in non ideal MHD approach. Simulation of plasma flow trajectories in tokamak like magnetic configuration with X-point is carried out. The method of plasma flow regulating in the vicinity of separatrix by varying divertor coil current is proposed. To sustain MHD simulation the impurity ion Newton-Lorentz simulations near X-point are carried out.

PACS: 52.55.Fa

1. MOTIVATION OF STUDY

A lot of experimental investigations on tokamaks are devoted to decreasing heat load on plasma faced components of the divertor and controlling impurity transport at plasma edge. The interest to this problem is caused by attempts to model fusion reactor scenarios on nowadays fusion devices. Method of X-point position sweeping is considered in framework of these studies.

In this paper a simple analytical model is proposed for analyzing the efficiency of the controlling the impurity ions with the divertor configuration. This approach is based on non ideal MHD consideration supplemented by single particle gyro-orbits simulation. The effect of vertical sweeping of the magnetic rib is considered for cylindrical geometry. The simplicity of magnetic configuration is provided by authors' wish to select the effect of X-point on plasma transport at the edge.

The simplest configuration (Fig. 1) is described in the Section 2. MHD fluxes are investigated in the Section 3. The dynamics of the impurity ions are considered in the Section 4. The principal conclusions are summarized in the Section 5.

2. MAGNETIC CONFIGURATION WITH X-POINT

Uniform magnetic field B_0 is parallel to z-axis and is maintained externally. Rotational transform of magnetic lines is created due to plasma current.

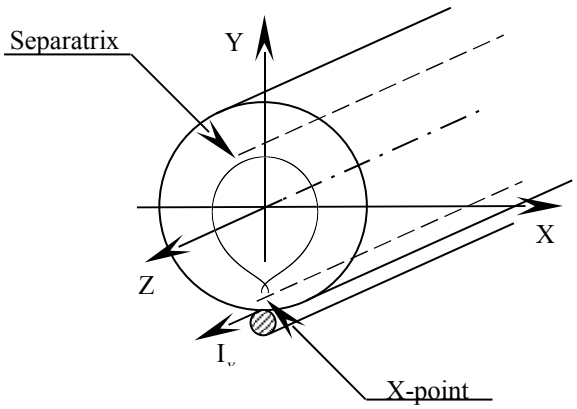

Fig.1. Magnetic field model

Assuming plasma current density $\mathbf{j}$ in following form

$$\mathbf{j} = j_0 \left(1 - \left(\frac{\Psi}{\Psi_b} \right)^{\alpha_j} \right) \mathbf{e_z}, \qquad (1)$$

where j_0 – plasma current density at magnetic axis, α_j - current density profile parameter, Ψ – magnetic surface function, $\Psi_b = \Psi\big|_{plasma\ edge}$, one can obtain components of magnetic field from following equation

$$\mathrm{rot}\,\mathbf{B} = \frac{4\pi}{c}\mathbf{j}, \qquad (2)$$

and then Ψ using

$$(\mathbf{B}\nabla\Psi) = 0. \qquad (3)$$

From the very beginning it is assumed that current is distributed uniformly $\mathbf{j}^{(0)} = j_0\mathbf{e_z}$. Thus we obtain

$$\mathbf{B}^{(0)} = B_0 \left\{ 0, \frac{r}{a}\iota^{(0)}, 1 \right\}, \qquad (4)$$

$$\Psi^{(0)} = b_0 \left(\frac{r}{a} \right)^2, \qquad (5)$$

where $b_0 = 2I_{\Sigma pl}/caB_0$ and $\iota^{(0)} = b_0 - const$ rotational transform angle, $I_{\Sigma pl}$ – net current, a – cylindrical vessel radius.

At next step of approximation it is assumed that plasma current density is distributed as in Eq. (1) with circular magnetic surfaces $\Psi^{(0)}$. Thus it is yield

$$\mathbf{B}^{(1)} = B_0 \left\{ 0, \frac{r}{a}\iota^{(1)}, 1 \right\}, \qquad (6)$$

$$\Psi^{(1)} = b_0 \left(\frac{r}{a} \right)^2 \left[1 + \frac{1}{\alpha_j} \left(1 - \frac{(r/a)^{2\alpha_j}}{\alpha_j + 1} \right) \right], \qquad (7)$$

where $\iota^{(1)} = b_0 + \left(b_0/\alpha_j\right)\left[1 - (r/a)^{2\alpha_j}\right]$.

For the next step approximation $\Psi^{(1)}$ can be substituted into Eq. (1) and then expressions for $\mathbf{B}^{(2)}$ and $\Psi^{(2)}$ can be obtained from Eqs. (2,3). We restrict ourselves to first approximation because obtained expressions give us satisfied description for magnetic field, in particular, parabolic profile for safety factor (rotational transform angle).

The linear current I_X is included to take into consideration the effect of divertor coils on magnetic configuration (see Fig.1). Components of magnetic field produced by this current are given by following expression

$$\mathbf{B}^{(X)} = \frac{B_0 b_X \{-\cos(\vartheta), (r/a + \sin(\vartheta)), 0\}}{1 + (r/a)^2 + 2(r/a)\sin(\vartheta)}. \quad (8)$$

Then substituting $\mathbf{B} = \mathbf{B}^{(1)} + \mathbf{B}^{(X)}$ in Eq. (3) and integrating it we obtain Ψ as $\Psi = \Psi^{(1)} + \Psi^{(X)}$, where

$$\Psi^{(X)} = \frac{1}{2} b_X \ln\left(1 + (r/a)^2 + 2(r/a)\sin(\vartheta)\right),$$

$$b_X = 2I_X / caB_0 . \quad (9)$$

It is convenient to normalize $\Psi^{(1)}$ in following way

$$\Psi_N(r,\vartheta) = \frac{\Psi(r,\vartheta) - \Psi(r_O,\vartheta_O)}{\Psi(r_X,\vartheta_X) - \Psi(r_O,\vartheta_O)}, \quad (10)$$

where r_O, ϑ_O and r_X, ϑ_X are coordinates of O-point (magnetic axis) and X-point (magnetic separatrix rib) respectively. It should be noted that after such procedure Ψ_N takes value '0' on magnetic axis and '1' on magnetic separatrix.

Radial profiles of $j_z(r,\vartheta_X)$ and $\Psi_N(r,\vartheta_X)$ are presented on Fig.2.

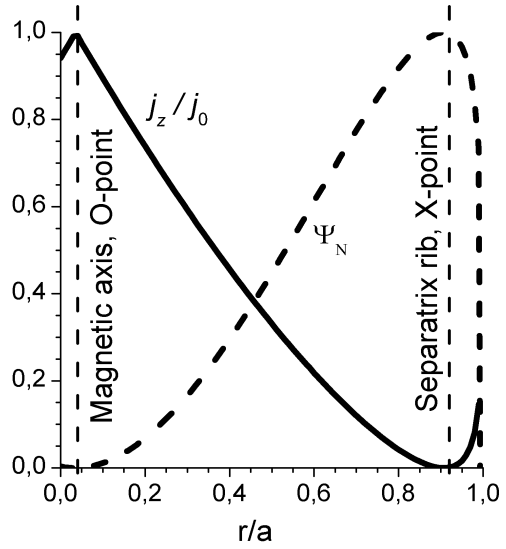

Fig.2. Radial profiles of $j_z(r,\vartheta_X)$ and $\Psi_N(r,\vartheta_X)$

For simulations following values for magnetic configuration parameters are used:
$B_0 = 3{,}4T$; $I_{\Sigma pl} = 2MA$; $\alpha_j = 0{,}5$; $I_X = 0{,}2MA$.

3. PLASMA MHD-FLOWS DISSIPATIVE MODEL

MHD approach is often used for treating impurity transport at the plasma edge.

3.1. TRANSPORT EQUATIONS

$$-\nabla p_a + e_a n_a \mathbf{E} + \frac{e_a n_a}{c}\mathbf{u}_a \times \mathbf{B} + \mathbf{F}_{a1} = 0, \quad (11)$$

$$-\frac{5}{2} n_a \nabla T_a + \frac{e_a n_a}{c}\frac{\mathbf{q}_a}{p_a} \times \mathbf{B} + \mathbf{F}_{a2} = 0, \quad (12)$$

with friction forces $\mathbf{F}_{a1}$ and $\mathbf{F}_{a2}$ taken in following form [3-4]

$$\mathbf{F}_{a1} = \sum_b l_{11}^{ab}\mathbf{u}_b + \frac{2}{5} l_{12}^{ab}\frac{\mathbf{q}_b}{p_b}, \quad (13)$$

$$\mathbf{F}_{a2} = \sum_b l_{21}^{ab}\mathbf{u}_b + \frac{2}{5} l_{22}^{ab}\frac{\mathbf{q}_b}{p_b}, \quad (14)$$

where a and b denote species of plasma component, p_a, n_a and T_a are the pressure, density and temperature of the plasma component a, e_a is the charge of the single plasma component a ion, $\mathbf{u}_a$ and $\mathbf{q}_a$ are particles and heat flows velocity of plasma component a, $\mathbf{E}$ and $\mathbf{B}$ are the electric and magnetic fields, l_{ik}^{ab} are the transport coefficients.

The transport coefficients l_{ik}^{ab} can be calculated with the use of technique proposed [1], and further developed in Refs [2-5].

3.2. TRANSPORT COEFFICIENTS

Further we consider a simple case of deuterium plasma containing a single species of impurity ion. For such case the analysis of the force balance was carried out by Rutherford [2] for a magnetic field model with circular magnetic surfaces. We suggest to analyze both force and thermal conduction equations in a same way because of theirs similarity. On this stage we don't assume any special magnetic field configuration.

For this case according to [3] transport coefficients could be expressed in such way

$$l_{11}^{DD} = -l_{11}^{DI} = -l_{11}^{ID} = l_{11}^{II} = l_1, \quad (15a)$$

$$l_{12}^{DD} = -l_{12}^{ID} = -l_{21}^{DI} = l_{21}^{DD} = l_2, \quad (15b)$$

$$l_{22}^{DD} = l_3, \quad (15c)$$

$$l_{12}^{DI} = l_{12}^{II} = l_{21}^{ID} = l_{21}^{II} = l_{22}^{DI} = l_{22}^{ID} = 0, \quad (15d)$$

$$l_1 = l_0 Z_{DI} C_1^*(Z_{DI}), \quad (16a)$$

$$l_2 = l_0 Z_{DI} C_2^*(Z_{DI}), \quad (16b)$$

$$l_3 = l_0 C_3^*(Z_{DI}), \quad (16c)$$

$$l_0 = \frac{m_D n_D}{\tau_{DD}} = 2{,}69 \cdot 10^{-7} \frac{\bar{n}_D^2 Z_D^4 M_D^{1/2}}{\bar{T}_D^{3/2}} \left[\frac{\mathrm{g \cdot cm^{-3}}}{\mathrm{sec}}\right], \quad (17)$$

$$\tau_{ab} = \frac{3}{4}\frac{m_a^{1/2} T_a^{3/2}}{\sqrt{2\pi}\, n_b e_a^2 e_b^2 \ln\lambda} = 6{,}22 \cdot 10^{-4} \frac{M_a^{1/2} \bar{T}_a^{3/2}}{\bar{n}_b Z_a^2 Z_b^2} [\mathrm{sec}]. \quad (18)$$

$\bar{n}_a = n_a / 10^{14}\,\mathrm{cm^{-3}}$ – normalized density; $\bar{T}_a$ – plasma temperature taken in *keV* units; M_a – mass number of species a. Effective charge number Z_{DI} is given by following expression $Z_{DI} = e_I^2 n_I / e_D^2 n_D$.

Coefficients $C_i^*(x)$ are obtained in [2] and can be obtained in a way which is shown in [3]:

$$C_1^*(x) = 0{,}48 + \frac{0{,}31}{0{,}59 + x}, \quad (19a)$$

$$C_2^*(x) = 0{,}3 + \frac{0{,}41}{0{,}59 + x}, \quad (19b)$$

$$C_3^*(x) = 1{,}13 + 0{,}5 \cdot x + \frac{0{,}55 \cdot x}{0{,}59 + x}. \quad (19c)$$

Index *D* denotes light ion (e.g. deuterium) and index *I* denotes impurity ion. Expressions (15), (16) and (19) are derived assuming $m_D << m_I$ (so called Lorentz collision model).

3.3. STATIONARY PLASMA MHD VELOCITIES

To obtain equations describing plasma transport parallel to magnetic field lines scalar products of Eqs. (11) and (12) with $\mathbf{B}$ are taken

$$l_1 U_{\parallel} + \frac{2}{5} l_2 \frac{q_{D\parallel}}{p_D} = -\nabla_{\parallel} p_D + e_D n_D (\mathbf{BE}), \quad (20a)$$

$$-l_1 U_{\parallel} - \frac{2}{5} l_2 \frac{q_{D\parallel}}{p_D} = -\nabla_{\parallel} p_I + e_I n_I (\mathbf{BE}), \quad (20b)$$

$$l_2 U_{\parallel} + \frac{2}{5} l_3 \frac{q_{D\parallel}}{p_D} = -\frac{5}{2} n_D \nabla_{\parallel} T_D, \quad (20c)$$

where subscript '||' denotes components parallel to magnetic field lines, $\mathbf{U} = \mathbf{u}_D - \mathbf{u}_I$ – relative velocity.

As it seen left hand parts of Eqs.(20a) and (20b) are equal up to minus sign that is why to have a solution right hand parts should satisfy such condition

$$-\nabla_{\parallel} p_D + e_D n_D (\mathbf{BE}) - \nabla_{\parallel} p_I + e_I n_I (\mathbf{BE}) = 0 \quad (21)$$

Integrating these equations taking into account condition (21) it is obtained

$$U_{\parallel} = \left(l_2^2 - l_1 l_3\right)^{-1} \left(\frac{l_3 \nabla_{\parallel} p_{eff}}{1 + (Z_I f_I)^{-1}} - \frac{5}{2} l_2 n_D \nabla_{\parallel} T_D \right). \quad (22)$$

If $p_D = p_D(\Psi)$, $p_I = p_I(\Psi)$, $T = T(\Psi)$ then

$$U_{\parallel} = 0, \text{ or } u_{D\parallel} = u_{I\parallel}. \quad (23)$$

To obtain equations for describing plasma transport across to magnetic field lines vector products of Eqs.(11) and (12) with $\mathbf{B}$ are taken. After integration of obtained equations it is yielded

$$\mathbf{u}_{D\perp} = \mathbf{v}_{dE} + \frac{1}{\rho_D \omega_D} \mathbf{h} \times \nabla p_D + \frac{1}{(\rho_D \omega_D)^2} \left(l_1 \nabla p_{eff} + l_2 n_D \nabla T_D \right), \quad (24a)$$

$$\mathbf{u}_{I\perp} = \mathbf{v}_{dE} + \frac{1}{Z_I f_I} \frac{1}{\rho_D \omega_D} \mathbf{h} \times \nabla p_I - \frac{1}{Z_I f_I} \frac{1}{(\rho_D \omega_D)^2} \left(l_1 \nabla p_{eff} + l_2 n_D \nabla T_D \right). \quad (24b)$$

In expressions (22) and (23) following designations are done: $\nabla p_{eff} = \nabla p_i - (Z_I f_I)^{-1} \nabla p_I$, $\omega_D = \frac{eB}{m_D c}$, $\rho_D = m_D n_D$, $\mathbf{v}_{dE} = \frac{c}{B^2} \mathbf{E} \times \mathbf{B}$, $\mathbf{h} = \mathbf{B}/B$.

Yielding Eqs.24 we neglect terms proportional $\left(l_{ik}^{ab}\right)^2$ because of its smallness in comparison to those taken into account. Such approach let us to analyze main transport processes in rather simple way. Considerable results were obtained with the use of this technique in [5-7].

3.4. PLASMA PARAMETERS AND ELECTRIC FIELD MODEL

First of all it is supposed that common temperature of deuterium and impurity plasma has been settled. Then it is assumed that plasma parameters depend on $\Psi_N(r,\vartheta)$ in following way

$$n_D = n_{DO}\left(1 - 0.7\Psi_N^{\alpha_{1nD}}\right)^{\alpha_{2nD}}, \quad (25a)$$

$$T = T_O\left(1 - 0.7\Psi_N^{\alpha_{1T}}\right)^{\alpha_{2T}}, \quad (25b)$$

$$n_I = n_{IX}\Psi_N^{\alpha_{nI}}, \quad (25c)$$

where n_D and n_I are plasma densities of deuterium and impurity respectively, T is plasma common temperature, α_i – are profile parameters, subscripts 'O' and 'X' denotes plasma parameters values on magnetic axis (O-point) and magnetic separatrix rib (X-point).

Numerical coefficient 0,7 is inputted in Eqs.(25) to describe non zero temperature and deuterium density beyond separatrix. After T, n_D and n_I are defined plasma component partial pressures are yielded in natural way

$$p_D = n_D kT, \quad (26a)$$

$$p_I = n_I kT. \quad (26b)$$

Radial profiles of plasma parameters at angle direction of X-point ($\vartheta = 3\pi/2$) are shown at Fig.3 for following profile parameters

$\alpha_{1nD} = 8$, $\alpha_{2nD} = 1$, $\alpha_{1T} = \alpha_{2T} = 1$, $\alpha_{nI} = 4$.

These profile parameters are used for further simulations with such values of

$n_{DO} = 10^{14}\,\text{cm}^{-3}$, $n_{IX} = 10^{13}\,\text{cm}^{-3}$ and $T_O = 20\,\text{keV}$.

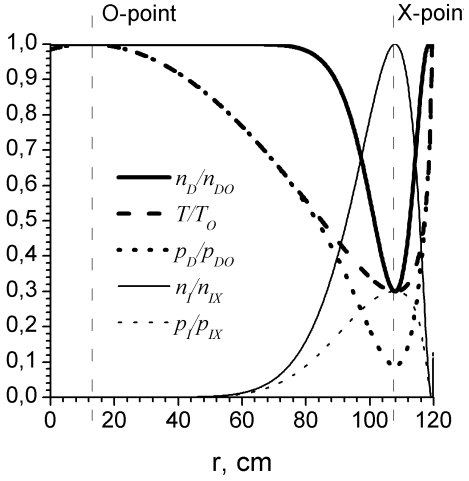

Fig.3. Radial profiles of plasma parameters at angle direction of X-point ($\vartheta = 3\pi/2$)

For electric potential following expression is used

$$\Phi_E = \Phi_{E0}\left(1 - \Psi_N^{\alpha_{1E}}\right)^{\alpha_{2E}}. \quad (27)$$

Electric field was defined as $\mathbf{E} = -\nabla \Phi_E$.

For further simulations such parameter values are used $\Phi_{E0} = -10\,\text{kV}$, $\alpha_{1E} = 8$ and $\alpha_{2E} = 1$.

3.5. FLOW TRAJECTORY SIMULATION RESULTS

To simulate flow trajectory we use following equation

$$d\mathbf{r} \times \mathbf{u}_{D,I} = 0 . \qquad (28)$$

In this section we try to simulate separatrix position varying. At Fig.4 flow trajectories of impurity plasma in deuterium plasma are shown in the vicinity of separatrix with the same start position in two magnetic configurations with $I_X = 0{,}2$ MA and $I_X = 0{,}22$ MA. Due to divertor coil current increasing separatrix is shifted inside. As it shown at Fig.4 separatrix Ψ_{X1} which corresponds to $I_X = 0{,}2$ MA is above start point and separatrix Ψ_{X2} which corresponds to $I_X = 0{,}22$ MA is under start point. This difference in initial conditions leads to increasing outside separatrix flow. Another aspect is that flow trajectories in both case don't differ much along separatrix and only near X-point flows deviates from each other (Fig.4,b) In first case flow stays in confinement volume and in second case flow moves out to imaginary divertor plate at position $r\sin(\vartheta) = -110$ cm under X-point ($r_X \sin(\vartheta_X) = -108$ cm).

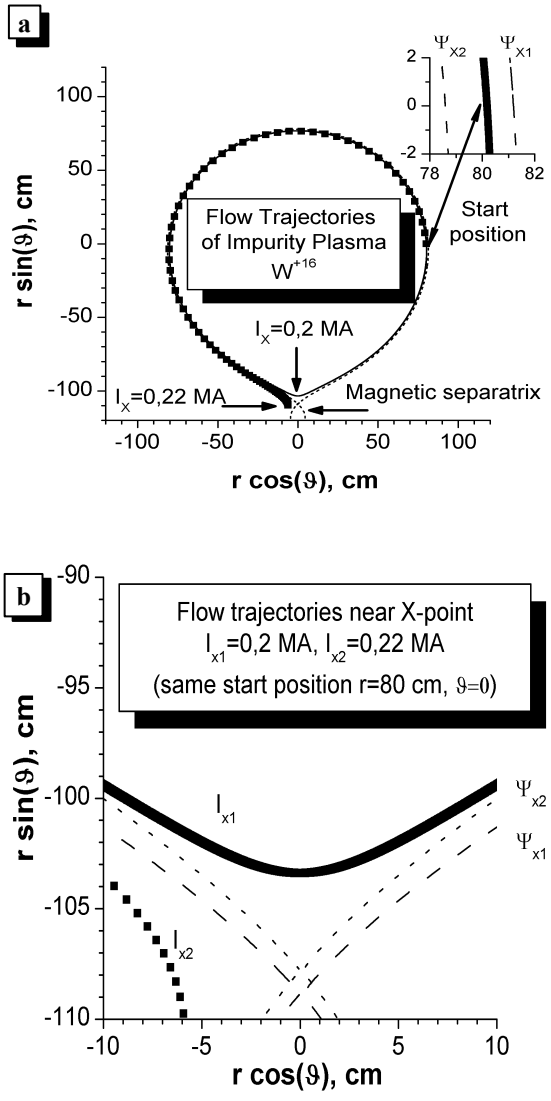

Fig.4. Flow trajectories of impurity plasma in deuterium plasma in the vicinity of separatrix with the same start position in magnetic configurations with $I_X = 0{,}2$ MA and $I_X = 0{,}22$ MA

At Fig.5 poloidal velocity of impurity plasma flow is presented. As it seen from Fig.5 poloidal velocity has the smallest value near X-point. On poloidal motion radial electric field plays the key role [9], [10]. As soon as electrostatic potential is function of Ψ at X-point E_r=0 because $\frac{\partial \Psi}{\partial r} = 0$.

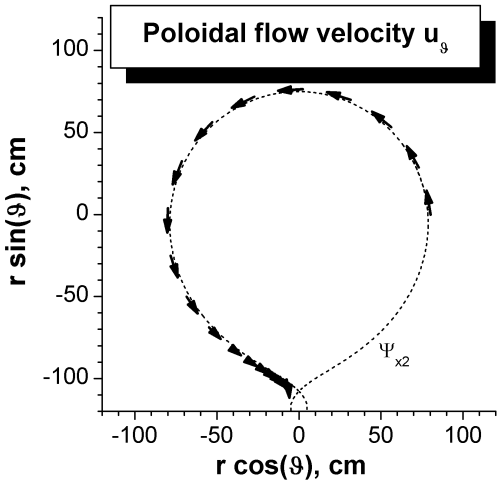

Fig.5. Poloidal flow velocity u_ϑ of impurity plasma flow in deuterium plasma in the vicinity of separatrix in magnetic configuration with $I_X = 0{,}22$ MA

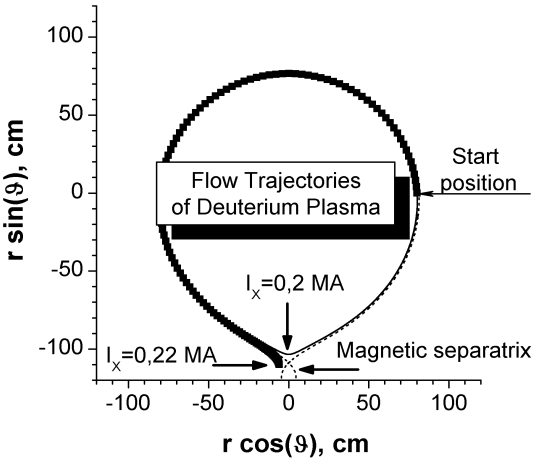

Fig.6. Flow trajectories of deuterium plasma in plasma with impurity (W^{+1}) in the vicinity of separatrix with the same start position in magnetic configurations with $I_X = 0{,}2$ MA and $I_X = 0{,}22$ MA

As it seen from Fig.6 deuterium plasma flow in the vicinity of separatrix don't differ from impurity plasma flow.

The effect of plasma flow escape due to divertor coil current increasing can be used as method of improving divertor regime. Application of similar technique on LHD (Japan) gives considerable results in long pulse experiments [8]. Efficiency of plasma edge refinement by X-point sweeping depends on impurity fraction at the plasma edge and current modulation.

4. SINGLE PARTICLE GYROORBIT MODEL

The MHD results obtained above can be supported with the single gyro-orbit particle motion simulation. We can see how the principle physics deduction based on MHD approach can be enriched with the single particle study. The particle trajectory due to drifts in the inhomogeneous magnetic and electric fields distinguishes from the magnetic surface. The consequences of this feature demonstrates itself in the different streamlines of the MHD flows and particle trajectories near separatrix.

4.1. NEWTON-LORENTZ EQUATION

For simulation ion gyro-orbit we use following equations

$$\frac{d\mathbf{r}}{dt} = \mathbf{v}, \tag{29}$$

$$\frac{d\mathbf{v}}{dt} = \frac{1}{m}\left(e\mathbf{E} + \frac{e}{c}\mathbf{v} \times \mathbf{B} \right), \tag{30}$$

where $\mathbf{r}$ and $\mathbf{v}$ are particle radius vector and velocity respectively, e and m are charge and mass of ion under consideration. Models for electric and magnetic field are used the same as in MHD approach.

For simulations we use tungsten ion W^{+16}. Tungsten is the most probable material of divertor face components. At the plasma edge charge number can be changed in wide range due to ionization/recombination processes.

4.2. SINGLE PARTICLE GYROORBIT SIMULATION RESULTS

On Fig.7 particle trajectory is presented. It is should be noted that due to drifts particle trajectory deflects from magnetic field line. As it shown on Fig.7,c magnetic field line escapes from confinement volume because its start position is above separatrix. In spite of start positions of magnetic field line and particle are the same (see Fig.7,b) particle stays in confinement volume. On Fig.7,b some simulation parameters are presented. $\Delta r_{start} = +0.01$ cm means that start position is 0.01 cm above separatrix. In presented case $\Delta r_{start} = \rho_L / 5$ where ρ_L is particle Larmor radius.

It should be noted that during motion ion crosses magnetic separatrix and become inside separatrix (Fig.7,c). Then it crosses separatrix once more and become outside separatrix. As it seen from Fig.7,b particle has done two full turns in poloidal direction and each time returns to its start position outside separatrix. Particle trajectory differs from magnetic field line due to drifts in inhomogeneous electric and magnetic fields

We'd like to mention that poloidal velocity of ion at start position is smaller than near X-point. Due to this effect near start position gyro-orbit spiral is seen well and near X-point only solid thick line is seen. As soon as space scale at Fig.7,b and Fig.7,c is the same it is possible to see that thickness of this thick line is about 2 Larmor radii. The same behavior of poloidal velocity is demonstrated above for plasma flow (Fig.5).

CONCLUSIONS. SIMULATION MODELS COMPARISON

Simple analytical non ideal MHD model is formulated. This model is applied for description of X-point sweeping effect on plasma flow near separatrix. It is demonstrated that it is possible to control plasma flow towards divertor plates by small variance of divertor coils (Fig.4).

The efficiency of such control could be investigated analytically for more complicate configurations with the help of proposed model.

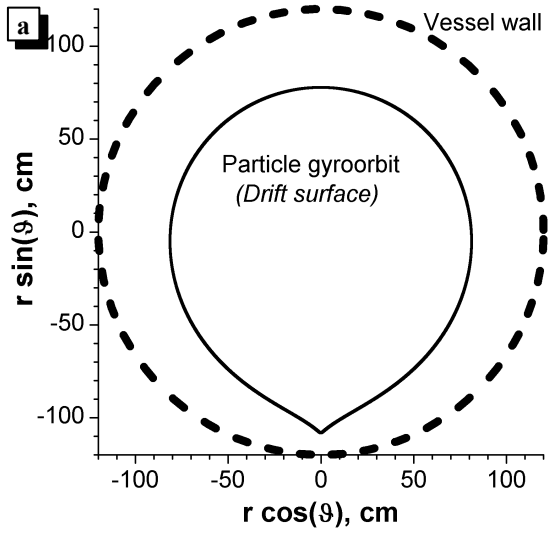

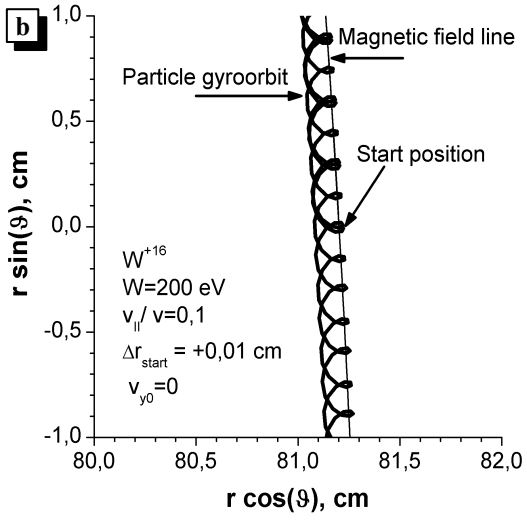

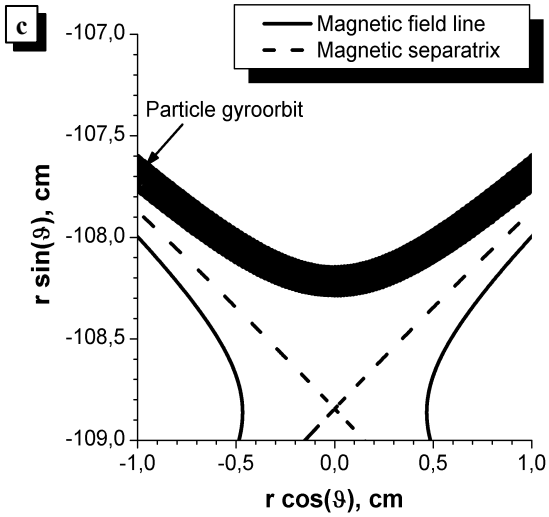

Fig.7. Single particle trajectory and magnetic field line which crosses particle orbit at start position in magnetic configuration with I_X = 0,2 MA
a)Full scale trajectory; b) enlarged fragment near start position; c) enlarged fragment near X-point

The results of single particle gyro-orbit motion simulation matches in main aspects with MHD-flows trajectories. As it seen from Fig.7 discrepancy is caused by drifts in the inhomogeneous magnetic and electric fields. MHD approach should be supplemented with Newton-Lorentz investigation of impurity ion motion near separatrix because near X-point even small variations in initial position and gyro phase defines escaping or penetration of ion under consideration.

ACKNOWLEDGMENTS

This work is supported by Science and Technology Center in Ukraine (Project 3685).

REFERENCES

1. S.I. Braginskii. Transport Phenomena in Plasma // *Reviews of Plasma Physics (edited by M.A.Leontovich)*. 1963, v.1, p.183-272.
2. P.H. Rutherford. Impurity transport in the Pfirsch-Schluter regime // *The Physics of Fluids*. 1974, v.17, №9, p.1782-1784.
3. S.P. Hirshman. Transport of a multiple-ion species plasma in the Pfirsch-Schluter regime // *The Physics of Fluids*. 1977, v.20, №4, p.589-598.
4. S.P.Hirshman, D.J.Sigmar. Neoclasical transport of impurities in tokamak plasmas // *Nuclear Fusion*, 1981, v.21, №9, p.1079-1201.
5. A.A. Shishkin. Impurity reversal in tokamak plasma with resonance magnetic fields due to local sources // *Nuclear fusion*. 1981, v.21, №5, p.603-607.
6. A.A. Shishkin. About the possibility of impurity ion accumulation in the island region in helical plasma // *Journal of plasma and Fusion Research SERIES*. 2004, v.6, p.500-503.
7. A.A. Shishkin, H.Mynik. Effect of magnetic islands on the impurity flows in NCSX geometry //*Problems of Atomic Science and Technology. Series «Plasma Physics»*. 2005, v.11, №2, p.23-25
8. Y. Nakamura, S. Masuzaki, T. Morisaki, et al. Impact of real-time magnetic axis sweeping on steady state divertor operation in LHD // *Nuclear Fusion*. 2006, v.46, №7, p.714-724.
9. D.Kh. Morozov, J.J.E. Herrera, V.A. Rantsev-Kartinov. Impurity penetration through the stochastic layer near the separatrix in tokamaks // *Physics of Plasmas*. 1995, v.2, №5, p.1540-1547.
10. V. Rozhansky, E. Kaveeva, S. Voskoboynikov, A.H. Bekheit, D. Coster, X. Bonnin, R. Schneider. Impact of E×B drifts on the distribution of impurities in the tokamak plasma edge // *Journal of Nuclear Materials*. 2003, 313-316, p.1141-1149.

Статья поступила в редакцию 08.05.2008 г.

ДИНАМИКА ПРИМЕСИ В МАГНИТНОЙ КОНФИГУРАЦИИ ТИПА ТОКАМАК С Х-ТОЧКОЙ

А.А. Москвитин, А.А. Шишкин

Получены выражения для скоростей потоков плазмы в инвариантной форме в приближении неидеальной МГД. Проведено моделирование траекторий потоков плазмы в магнитной конфигурации типа токамак с Х-точкой. Предложен метод регулирования потока плазмы на диверторные пластины путем изменения тока в диверторных проводниках. Для подтверждения МГД-моделирования было проведено Ньютон-Лоренц-моделирование примесного иона вблизи Х-точки.

ДИНАМІКА ДОМІШКИ В МАГНІТНІЙ КОНФІГУРАЦІЇ ТИПУ ТОКАМАК З Х-ТОЧКОЮ

А.О. Москвітін, О.О. Шишкін

Отримано вирази для швидкостей потоків плазми в інваріантній формі у наближені неідеальної МГД. Проведено моделювання траєкторій потоків плазми в магнітній конфігурації типу токамак з Х-точкою. Запропоновано метод регулювання потоку плазми на диверторні пластини шляхом змінювання струму в диверторних провідниках. Для підтвердження МГД-моделювання було проведено Ньютон-Лоренц-моделювання иона домішки поблизу Х-точки.